View metadata, citation and similar papers at core.ac.uk

brought to you by CORE

provided by Elsevier - Publisher Connector

Available online at www.sciencedirect.com

ScienceDirect

Procedia Materials Science 3 (2014) 1606 – 1611

Procedia Materials Science

www.elsevier.com/locate/procedia

20th European Conference on Fracture (ECF20)

Unified characterization of crack growth parameters based on plastic stress intensity factor

V.N. Shlyannikov*, N.V.Boychenko, A.V.Tumanov and A.P. Zakharov

Research Center for Power Engineering Problems of the Russian Academy of Sciences
Lobachevsky street, 2/31, post-box 190, Kazan, 420111, Russia

Abstract

The aim of this work is to study and represent the combined in-plane and out-of-plane constraint effect on the material fracture resistance characteristics under static and fatigue loading. Subjects for numerical and experimental studies are three-point bending and compact specimens under static loading as well as cruciform specimens under cyclic biaxial and mixed mode loading. For the static tests experimental specimen geometries considered (SENB and CS), the elastic constraint parameters and the parameter governing of the plastic stress field I_n distributions are obtained as a function of both the specimen thickness, the dimensionless crack length and crack length. For the fatigue tests specimen configurations (CCS) the T-stress and the numerical constant I_n are calculated with the variation of biaxial stress ratio and full range mode mixity. A method is also suggested for calculating the plastic stress intensity factor for mixed-mode I/II loading based on the T-stress and power law solutions. It is found that the plastic stress intensity factor accounting for the in-plane and out-of-plane constraint effect can be applied to characterize the fracture toughness and the multiaxial crack growth rate for a variety specimen geometries.

© 2014 Published by Elsevier Ltd. Open access under CC BY-NC-ND license.
Selection and peer-review under responsibility of the Norwegian University of Science and Technology (NTNU), Department of Structural Engineering

Keywords: plastic stress intencity factor ; in-plane constraint; out-of-plane-constraint; static loading; fatigue;

1. Introduction

The engineering application of the fracture mechanics of solids to real cracked structures requires an appropriate parameter to quantify the crack tip constraint. Moreover, practical structural components have finite thicknesses, and the stress-strain state changes between plane stress and plane strain. From a practical point of view, the most useful

* Corresponding author. Tel.: +7-843-2363102; fax: +7-843-2363102.
E-mail address: shlyannikov@mail.ru

2211-8128 © 2014 Published by Elsevier Ltd. Open access under CC BY-NC-ND license.
Selection and peer-review under responsibility of the Norwegian University of Science and Technology (NTNU), Department of Structural Engineering
doi:10.1016/j.mspro.2014.06.259

approach for assessing the fracture resistance of materials, components and structures would involve one common parameter, which, unlike the two parameter models and the higher order term solutions, would preserve the one-term representation. Nevertheless, the basic parameters of the model must be modified such that they are able to take into account both the in-plane and out-of-plane constraint effects.

Hutchinson (1968) and Hilton and Hutchinson (1971) suggested the use of the elastic-plastic stress intensity factor (SIF) as the amplitude of the first term for pure mode I of the asymptotic stress expansion. According to this approach, the plastic stress intensity factor (SIF) can be expressed directly in terms of a corresponding elastic stress intensity factor using Rice's J-integral. Hutchinson and Hilton (1968,1971) have introduced critical values for the plastic SIFs associated with fracture initiation as a direct analog to elastic fracture mechanics. In the small-scale yielding range, when elastic and plastic SIFs are directly related to each other, the predictions based on the plastic SIFs are identical to those based on the elastic SIFs.

In the classical first-term singular HRR-solution, the numerical parameter In is a function of only the material strain hardening exponent n. Shlyannikov and Tumanov (2014) reconsidered the HRR-solution for both plane strain and plane stress and supposed that under small-scale yielding, the expression for I_n depends implicitly on dimensionless crack length and specimen configuration. The authors supposed that for moderate large-scale yielding conditions or plastic deformations, instead of using the two parameter approaches, the fracture process can be controlled by using a single parameter in the form of an elastic-plastic stress intensity factor and that this one-parameter approach is sensitive to the in-plane and out-of-plane constraint effects.

The applicability of the plastic stress intensity factor to analyze the in-plane and out-of-plane constraint effects is studied in the present work in the terms of the fracture toughness. The plastic SIF approach originally proposed to describe fracture toughness for pure mode I under monotonic/static loading, is also employed to study the crack growth rate under cyclic biaxial and mixed mode fracture.

2. Theoretical background

The current study explores the direct use of elastic-plastic FEM analysis for calculating the plastic SIFs in various specimen geometries. According to the method suggested by Shlyannikov and Tumanov (2014), the numerical values of the plastic stress intensity factors K_P can be determined as follows

$$K_P = \left[\frac{K_{1i}^2(a/w)}{\overline{\alpha}\sigma_0^2 I_n^{FEM}\left[\theta,(a/w),(z/B)\right]} \right]^{1/(n+1)} ; \quad K_P = \left[\left(\frac{\sigma}{\sigma_o} \right)^2 \frac{\left(K_1^2(\overline{T}) + K_2^2(\overline{T})\right)}{\overline{\alpha} I_n^{FEM}\left(\theta, n, M_P, (a/w)\right)} \right]^{1/(n+1)} \tag{1}$$

where K_i is elastic stress intensity factors, I_n is numerical constant, σ_0 is yield stress, $\overline{\alpha}$ and n are strain hardening parameters, M_P is mode mixity parameter, a/w is relative crack length, z/B is relative thickness, $\overline{T}$ is dimensionless T-stress. The use of the Hutchinson's (1968) theoretical definition for the governing I_n-factor of the elastic-plastic stress fields directly adopted in the numerical finite element analyses leads to Shlyannikov and Tumanov (2014) in polar coordinates r, θ

$$I_n^{FEM}\left(\theta, M_p, n, (a/w)\right) = \int_{-\pi}^{\pi} \Omega^{FEM}(\theta, M_P, n, (a/w)) d\theta \tag{2}$$

$$\Omega^{FEM}\left(\theta, M_P, n, (a/w)\right) = \frac{n}{n+1}\left(\widetilde{\sigma}_e^{n+1}\right)^{FEM}\cos\theta - \left[\widetilde{\sigma}_{rr}^{FEM}\left(\widetilde{u}_\theta^{FEM} - \frac{d\widetilde{u}_r^{FEM}}{d\theta} \right) - \widetilde{\sigma}_{r\theta}^{FEM}\left(\widetilde{u}_r^{FEM} + \frac{d\widetilde{u}_\theta^{FEM}}{d\theta} \right) \right]\sin\theta -$$

$$- \frac{1}{n+1}\left(\widetilde{\sigma}_{rr}^{FEM}\widetilde{u}_r^{FEM} + \widetilde{\sigma}_{r\theta}^{FEM}\widetilde{u}_\theta^{FEM}\right)\cos\theta.$$

In such a case, the numerical integral of the crack tip field I_n not only changes with the strain hardening exponent n but also changes with the relative crack length a/w , the crack angle and the specimen configuration.

3. In - factor distributions

The subjects in both experimental studies and numerical analyses are the single-edge-notched bend (SENB), compact (CS) and cruciform (CCS) specimens which the loading configuration and geometry shown in Fig. 1.

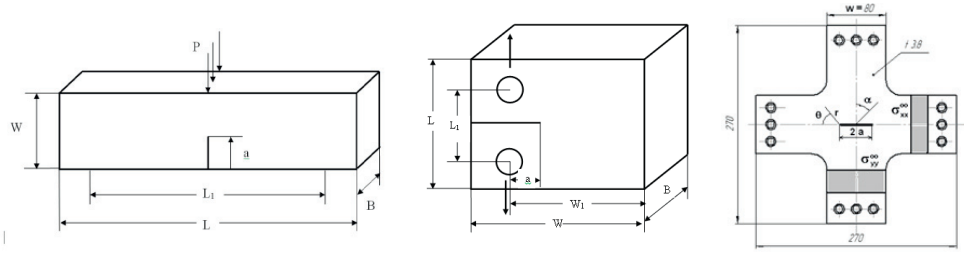

Fig.1. SENB, CS and CCS specimens.

Both SENB and CS specimens are produced in carbon steel 34XH3MA while CCS specimens manufactured in structural steel 3, whose main mechanical properties are listed in Table 1.

Table 1. Main mechanical properties

Specimen configuration	Material	Young modulus E (MPa)	Yield stress σ_0 (MPa)	Ultimate stress σ_f (MPa)	Strain hardening exponent n	Strain hardening coefficient $\overline{\alpha}$
SENB, CS	steel 34XH3MA	196363	790	991.9	7.300	2.4568
CCS	steel 3	207985	293	580.1	3.142	15.135

The expressions for elastic stress intensity factors K_1 and K_2 for CS, CTS and CCP as a function of geometry-dependent correction factors Y_1 and Y_2 (as a consequence of the T-stress and the relative crack length) are given by Eqs. (3,4)

For CCS: $$K_1(T)=\frac{\sigma\sqrt{\pi a}}{2}\left[(1+\eta)-(1-\eta)\cos 2\alpha\right]Y_1\left(\frac{a}{w},\alpha,\overline{T}\right);\quad K_2(T)=\frac{\sigma\sqrt{\pi a}}{2}\left[(1-\eta)\sin 2\alpha\right]Y_2\left(\frac{a}{w},\alpha,\overline{T}\right) \tag{3}$$

for SENB: $$K_{1B}=\sigma_B\sqrt{\pi\lambda}\left(Y_{1B}/\sqrt{\pi}\right),\ \sigma_B=\frac{6M}{Bw^2},\ \lambda=a/w;\quad \text{for CS: } K_{1CS}=\sigma_{CS}\sqrt{\pi\lambda}\left(Y_{1CS}/\sqrt{\pi}\right),\ \sigma_{CS}=\frac{P}{Bw} \tag{4}$$

By fitting the numerical calculations, the constraint parameter $\overline{T}$ -stress and the geometry dependent correction factors Y_1 and Y_2 as function of the crack length and crack angle for the particular geometry considered have been represented in the form of polynomial equations. The equations for these factors in terms of geometrical parameters are given by Shlyannikov (2013).

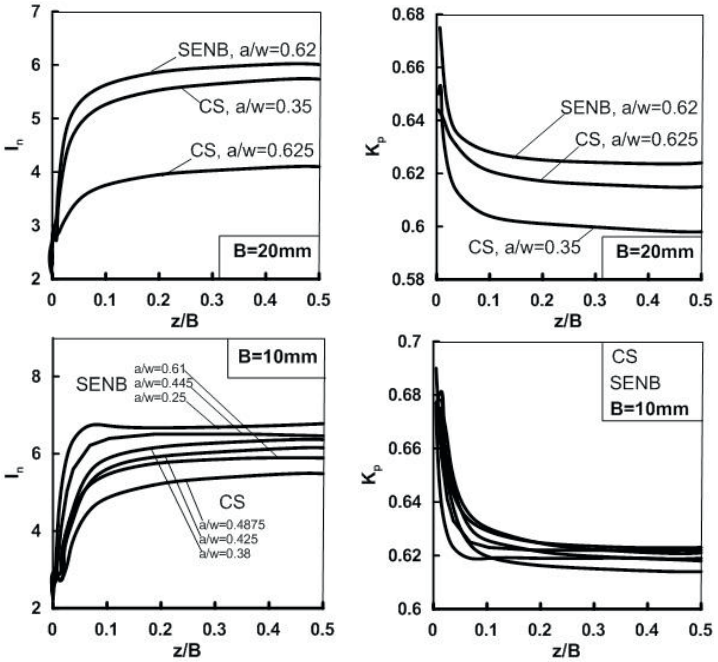

Fig.2. In – factor and plastic SIF distributions along crack front for SENB and CS.

Full-field elastic-plastic FEA are performed using ANSYS finite element (FE) code to study the constraint effect on the crack-front stress fields for SENB and CS specimens of various configurations. The FE calculations re used the J_2 incremental theory of plasticity.

Figure 2 shows an example of varying the I_n -factor and the plastic SIF K_P along the 3D crack-front at the transition from plane stress to plane strain in SENB and CS specimens, whereas the proportional coefficient in Eq. (1), I_n, is affected by the stress constraint. To calculate the plastic SIFs K_P for the specimen-specified geometry, the expression for the I_n-factor in the form of Eq. (2) as well as the values of the limiting experimental loads P_{max} was used. Figure 2 presents for the SENB and CS geometries a clear illustration of the influence of the in-plane and out-of-plane constraint effects on the I_n-factor behavior. The numerical results concerning the I_n-distributions in the SENB and CS in the range between the plane stress and the plane strain indicates the obvious potential of the in-plane and out-of-plane constraint interaction as a function of the tested specimen configuration. Note that the K_P -curves as a function of the relative crack length and specimen thickness in the mid-plane are close to each other for the different specimen geometries.

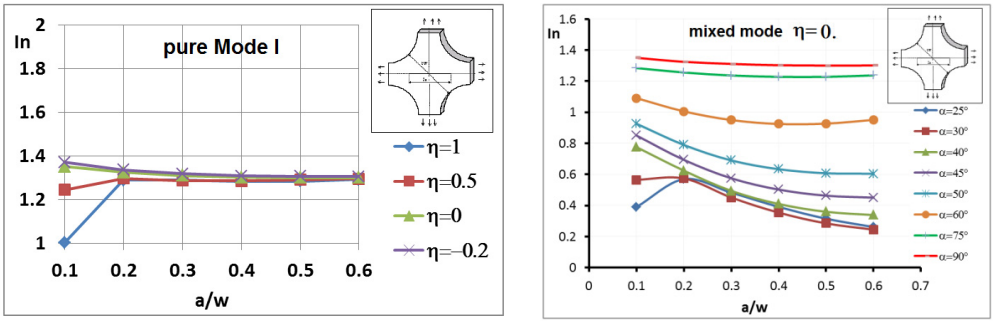

a) b)

Fig.3. In – factor distributions under biaxial loading for CCS .

The values of the numerical constant of the elastic-plastic stress field in the form of the I_n-integral are calculated for the cruciform specimens at different combinations of load biaxiality and mode mixity, keeping in mind that the dimensionless angular stress $\tilde{\sigma}_{ij}^{FEM}$ and displacement $\tilde{u}_i^{FEM}$ functions are directly determined from the FEA distributions. Figure 3,a presents for the CCS geometry It is interesting to note that the I_n-curves as a function of load biaxiality are close to each other for the same specimen geometries. Figure 3,b shows the relationship between the I_n-integral and the relative crack length a/w under plane stress mixed mode fracture for CCS specimen configuration with load biaxiality $\eta = 0$. This figure gives a clear illustration of the influence of mode mixity under the biaxial loading on the I_n-factor plane stress behavior. As expected, although it is not shown here, the computed values of the I_n-integral are sensitive to a general state of either plane stress or plane strain conditions.

4. Experimental results of crack growth

4.1. *Static loading*

The SENB and CS test specimen configurations were designed basically in accordance with ASTM E399 (2005). In addition to the standard ASTM thickness-to-width ratio $B/W = 0.5$, SENB specimens with $B/W = 1.0$ were prepared. The relative crack length a/W after inserting a fatigue precrack varied in the range of 0.3-0.62. The three type of CS specimens with the ratio $B/W = 0.1$, 0.2, and 0.4 were chosen with the relative crack length a/W change of 0.35-0.645 after pre-cracking.

In Fig. 4 shown the experimental results for steel 34XH3MA where the values of plastic SIF correspond to the mid-plane of each specimen at $z/B = 0.5$. It can be seen that in contrast to the elastic SIF, the distributions of plastic SIF K_P as a function of relative crack length and specimen thickness exhibited a lower scatter average to $K_P \cong 0.61$. Furthermore, this value of K_P is independent of the considered specimen geometry, i.e., it is a material characteristic. Thus, the plastic stress intensity factor K_P in the formulation of Eq. (1) may treated as a unified parameter for the characterization of the material fracture resistance property.

A one-parameter approach based on the plastic stress intensity factor, K_P, can be more convenient for practical use in assessing the fracture resistance under monotonic and cyclic loading of materials and structural elements. In fact, Eqs. (1) refers to the formulation of the requirement of the one-parameter approach. Thus, accounting for the in-plane constraint effect is fully implemented through the geometry-dependent correction factor $Y_1(a/w)$, which is

an implicit function of the *T*-stress. Three-dimensional effects associated with the out-of-plane constraint in the thickness direction are implemented in Eqs. (1) through the constant of integration I_n in form of Eq. (2), for instance

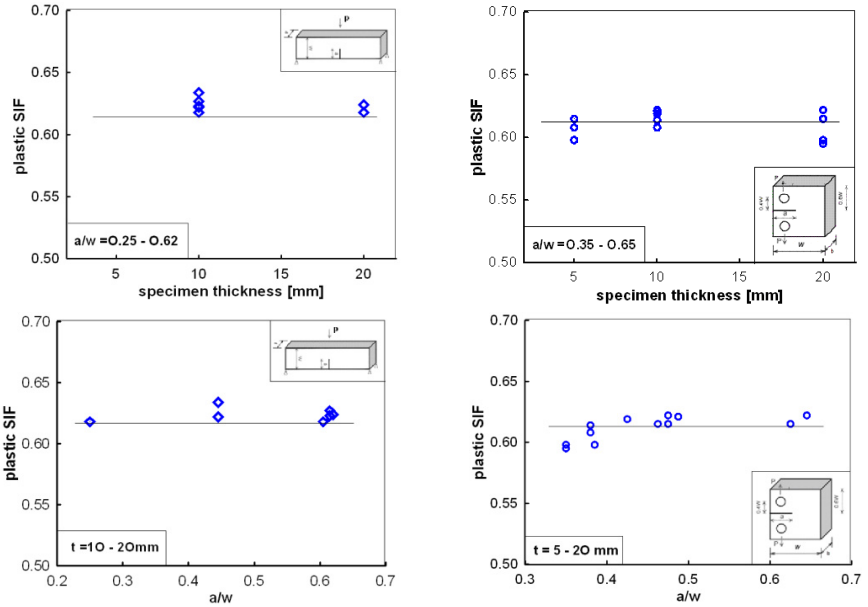

Fig.4. Variation of plastic SIF's as a function of SENB and CS specimen thickness and relative crack length.

for the SENB and CS configurations. With a simple definition and with no additional assumptions, the plastic stress intensity factor can also characterize 3D crack tip fields and control 3D fracture. The decisive argument for the choice of the fracture parameter is the sensitivity of K_P through the I_n values to in-plane and out-of-plane constraint effects.

4.2. *Cyclic loading*

The experimental study of fatigue crack growth rate in steel 3 is performed on biaxially loaded cruciform specimens with thickness 3.8 mm. All specimens for biaxial loading contained through thickness central cracks with initial size equal to 20mm. A series of tests were performed to study the effect of the tension-compression loading biaxiality on crack growth rate in the same configuration of cruciform specimens under pure mode I. The range of nominal stress σ^{∞}_{yy} was kept constant throughout a test series, while σ^{∞}_{xx} was varied for four different forms of test. The stress state designated through η, equal to the ratio of σ^{∞}_{xx} and σ^{∞}_{yy}, (where the latter two terms are the maximum values of stress in a cycle), has been assumed equal to +1.0, +0.34, -0.2 and -0.4. The investigation of fatigue mixed mode crack growth rate in CCS specimens was performed under biaxial loading with ratio $\eta = 0$. The original crack has angle α with respect to the loading direction. Different combinations of Modes I and II are achieved due to changing of α-angle. In the CCS under biaxial loading $\eta = 0$, angle $\alpha = 90^{\circ}$ corresponds to pure mode I, and pure mode II can be achieved when $\alpha = 25^{\circ}$.

In the all considered cases, the maximum applied stress and the R-ratio were the same with only the biaxiality ratio η being varied. The CCS fatigue crack growth tests have been carried out on a special servohydraulic biaxial test facility with frequency 5 Hz at stress ratio R=0.1. Tensile or compressive loads are applied to each pair of arms of a cruciform specimen (Fig. 1), developing a biaxial stress field in the working section. The loads are controlled such that specified forces are produced on opposing arms of the CCS according to given load biaxiality.

An addition to the traditional interpretation of the cyclic fracture resistance characteristic of the materials as (*da/dN*) vs the elastic SIF, in Fig.5a the multiaxial crack growth results are presented in terms of crack growth rate plotted against the plastic stress intensity factor K_P for tested CCS specimen geometries. An obvious trend of the influence of biaxiality on crack growth rate is seen for the CCS in terms of the plastic SIF. The biaxilal loading effect of lower growth rate when η is negative is observed. Figure 5b presents data similar to those of Fig. 5a, but for cyclic mixed mode fracture. It is found that the pure Mode I cracks clearly propagate more rapidly than in the mixed mode cases. Looking at Fig.3 and considering general changes in the I_n - factor distributions under the same stress amplitude applied to the CCS specimens in pure Mode I and pure Mode II, significant differences in the crack

growth rate under the above types of loading conditions are expected. A wide range of the fatigue fracture diagram variation in Fig.5b depending to the behavior of governing elastic-plastic stress field parameter I_n represented in Fig. 3 from pure Mode I to pure Mode II are shown. Unlike the elastic SIF, plastic stress intensity factor K_P in the formulation of Eq. (1) is enough sensitive to account for the influence of the specimen geometry (including of thickness), load biaxialities and the mixed mode loading conditions.

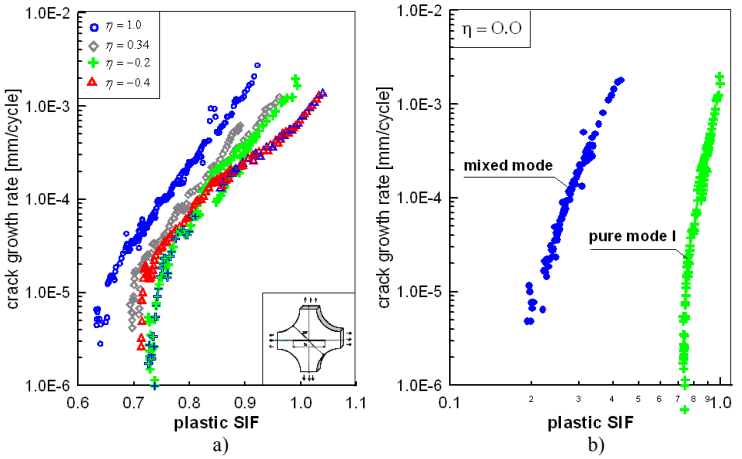

Fig.5. Crack growth rate as a function of plastic SIF's under (a) pure mode I and (b) mixed mode fracture.

In the well-known equation of Paris, describing a linear part of the fatigue fracture diagrams represented through the crack growth rate *da/dN* versus the elastic SIF, the parameters *C* and *m* can be considered as constants to characterize the material resistance to crack growth under cyclic loading. Analogously in the small-scale yielding range, when the plastic SIF is the governing parameter of cyclic fracture, the predictions based on the plastic SIFs are similar to those based on the elastic SIFs in the form of fatigue fracture diagram (*da/dN* vs plastic SIF) with another parameters C_P and m_P.

There are very obvious advantages when using the plastic SIF to characterize the material's resistance to cyclic crack growth. For instance, practical structural components have finite thicknesses, and the stress-strain state changes between plane stress and plane strain. However, it is well known that the elastic SIFs have the same values for these situations at the specified nominal stress level. Contrary to that, as expected, the computed values of the plastic SIFs are sensitive to a general state of either the plane stress or plane strain conditions. Moreover, the numerical results from the present study concerning the I_n-distributions in Fig.2 for both the SENB and CS in the range between the plane stress and the plane strain indicates the obvious potential of the plastic SIF to describe the influence of the in-plane and out-of-plane constraint interaction on the crack growth rate as a function of the tested specimen configuration.

The purpose of this work is to pay attention on various forms of the elastic and plastic constraint parameter applications to the analysis of static and fatigue crack propagation. Distinctions in the behavior of the in-plane and out-ot-plane constraint parameters along crack front towards the thickness of the tested specimens have been observed under bending and tension loading conditions of power law hardening material for various configurations of the SENB and CS. The experimental results of the present study gave the opportunity to explore the suggestion that fracture toughness and multiaxial fatigue crack propagation may be governed more strongly by the plastic stress intensity factor rather than the magnitude of the elastic SIFs alone. The I_n-factor is used as the main parameter of the elastic-plastic stress intensity factor, which is sensitive to the in-plane and out-of-plane constraint effects.

Acknowledgements

The author gratefully acknowledges the financial support of the Russian Foundation for Basic Research under the Project 12-08-97085p.

References

Hutchinson, J., 1968. Singular behavior at the end of a tensile crack in a hardening material. Journ. Mech. Phys. Solids. 16, 13-31.

Hilton, P., Hutchinson, J., 1971. Plastic Intensity Factors for Cracked Plates. Engineering Fracture Mechanics 3, 435-451.

Shlyannikov, V., Tumanov, A., 2014. Characterization of crack tip stress fields in test specimens using mode mixity parameters. Int. J. Fracture 185, 49-76.

Shlyannikov, V., 2013. T-stress for crack paths in test specimens subject to mixed mode loading. Engng. Fract. Mech. 108, 3-18.

ASTM E399-05, 2005. Standard test method for plane strain fracture toughness of metallic materials.Annual book of ASTM standards.